J Neurooncol
DOI 10.1007/s11060-017-2420-1

LABORATORY INVESTIGATION

Radiogenomics of lower-grade glioma: algorithmically-assessed tumor shape is associated with tumor genomic subtypes and patient outcomes in a multi-institutional study with The Cancer Genome Atlas data

Maciej A. Mazurowski[1,2,3] · Kal Clark[1] · Nicholas M. Czarnek[2] · Parisa Shamsesfandabadi[1] · Katherine B. Peters[4] · Ashirbani Saha[1]

Received: 24 October 2016 / Accepted: 9 April 2017

Abstract Recent studies identified distinct genomic subtypes of lower-grade gliomas that could potentially be used to guide patient treatment. This study aims to determine whether there is an association between genomics of lower-grade glioma tumors and patient outcomes using algorithmic measurements of tumor shape in magnetic resonance imaging (MRI). We analyzed preoperative imaging and genomic subtype data from 110 patients with lower-grade gliomas (WHO grade II and III) from The Cancer Genome Atlas. Computer algorithms were applied to analyze the imaging data and provided five quantitative measurements of tumor shape in two and three dimensions. Genomic data for the analyzed cohort of patients consisted of previously identified genomic clusters based on IDH mutation and 1p/19q co-deletion, DNA methylation, gene expression, DNA copy number, and microRNA expression. Patient outcomes were quantified by overall survival. We found that there is a strong association between angular standard deviation (ASD), which measures irregularity of the tumor boundary, and the IDH-1p/19q subtype ($p < 0.0017$), RNASeq cluster ($p < 0.0002$), DNA copy number cluster ($p < 0.001$), and the cluster of clusters ($p < 0.0002$). The RNASeq cluster was also associated with bounding ellipsoid volume ratio ($p < 0.0005$). Tumors in the IDH wild type cluster and R2 RNASeq cluster which are associated with much poorer outcomes generally had higher ASD reflecting more irregular shape. ASD also showed association with patient overall survival ($p = 0.006$). Shape features in MRI were strongly associated with genomic subtypes and patient outcomes in lower-grade glioma.

Keywords Lower-grade gliomas · Tumor shape feature · Tumor genomic subtype · Radiogenomics · Brain MRI

✉ Maciej A. Mazurowski
maciej.mazurowski@duke.edu

Kal Clark
kal.clark@dm.duke.edu

Nicholas M. Czarnek
nicholas.czarnek@duke.edu

Parisa Shamsesfandabadi
parisa.shamsesfandabadi@duke.edu

Katherine B. Peters
katherine.peters@duke.edu

Ashirbani Saha
as698@duke.edu

[1] Department of Radiology, Duke University, Durham, NC, USA

[2] Department of Electrical and Computer Engineering, Durham, NC, USA

[3] Duke Medical Physics Program, Durham, NC, USA

[4] Department of Neurology, Durham, NC, USA

Introduction

Lower-grade gliomas are a group of WHO grade II and grade III brain tumors including well-differentiated and anaplastic astrocytomas, oligodendroglimas, and oligoastrocytomas [1, 2]. While patients with lower-grade gliomas can have median overall survival measured in years or even decades, some of these tumors can transform into glioblastomas [3], which are associated with a very grim overall survival of approximately 10% at 5 years [4]. Treatment for lower-grade gliomas is varied and remains not standardized, and the current histopathological classification is inaccurate at predicting patient outcomes and associated with inter-observer variability [1]. Therefore, new classification systems that distinguish patients with different

Published online: 03 May 2017

outcomes are in urgent need. Although utilization of telomerase reverse transcriptase promoter (TERT) mutation status, isocitrate dehydrogenase (IDH) mutation status, and 1p/19q co-deletion is now increasingly used to prognosticate [5], more is needed to understand what drives different outcomes for these patients.

Recent genomic analyses have focused on identifying distinct subgroups of lower-grade gliomas [1, 5–8]. Specifically, Brat et al. [1] identified distinct subtypes of LGGs through clustering of the tumors based on DNA methylation, gene expression, DNA copy number, and microRNA expression, which were largely concordant with a basic molecular subtype based on IDH (IDH1 or IDH2) mutation and 1p/19q co-deletion [1, 6]. Patients belonging to different molecular groups showed a dramatically different typical course of the disease. In another recent study [5], the authors defined five glioma subtypes based on IDH mutation, 1p/19q co-deletion, and mutations in the TERT promoter and showed that they differ in terms of age at onset and overall survival.

Recently, a new research direction in cancer has emerged that aims at investigating the relationship between tumor genomic characteristics and its presentation in medical imaging, i.e., its radiophenotype. This direction is often referred to as radiogenomics or imaging genomics [9]. While very recent radiogenomic discoveries appeared in the literature on other tumors [9–17] radiogenomics of lower-grade gliomas is still virtually untouched.

Radiogenomic analysis in lower-grade glioma is of high significance. First, since the molecular classification of LGGs is still new, correlating molecular subtypes with different imaging presentation would provide an additional level of validation to such classification. Second, advanced imaging features that go beyond our current imaging assessment paradigm [18] could provide a non-invasive surrogate or alternative classification to genomic analysis. Imaging features could also provide complementary information that could in turn result in a hybrid genomic-imaging classification. Finally, radiogenomic analysis will provide a better understanding of underlying genomic characteristics of different growth patterns.

In this study, we analyzed the association of tumor genomic subtypes based on four platforms (DNA methylation, gene expression, DNA copy number, and microRNA expression), cluster of clusters analysis, and a basic IDH-1p/19q subtype with quantitative imaging features. The imaging features are extracted using computer algorithms to quantify 2D and 3D shape of the tumor. To our knowledge, this is the first study on radiogenomics in lower-grade gliomas. We also assessed the association of the quantitative imaging features with outcomes. We presented the preliminary results on the association of lower grade gliomas with shape features in Mazurowski et al. [19]

Methods

Patient population

This was a study of publicly available data from The Cancer Genome Atlas (TCGA). We secured an institutional review board exemption for studying this data at our institution. In the TCGA lower-grade glioma collection, we identified 120 patients that had preoperative imaging data available that contained a fluid-attenuated inversion recovery (FLAIR) sequence. Out of these, we excluded ten patients that did not have genomic cluster information available for any of the analyzed clusters which resulted in 110 patients used for the analysis. The patients from the analyzed group were from five institutions: Thomas Jefferson University (TCGA-CS, 16 patients), Henry Ford Hospital (TCGA-DU, 45 patients), UNC (TCGA-EZ, 1 patient), Case Western (TCGA-FG, 14 patients), Case Western-St. Joseph's (TCGA-HT, 34 patients) from TCGA LGG collection. The full list of patients used is shown in Appendix 1.

Imaging data

Imaging data was downloaded from The Cancer Imaging Archive (TCIA), which contains the medical imaging data counterpart for the TCGA patients and is sponsored by the National Cancer Institute. We analyzed preoperative data for patients that had a preoperative FLAIR sequence. FLAIR sequences are typically acquired in brain imaging patients and provide a clear assessment of the extent of the tumor. This study used FLAIR, rather than enhancing tumor, abnormality as the basis of assessing tumor shape since enhancement in lower grade gliomas, unlike in GBMs, is rare. We analyzed only preoperative data to capture the original pattern of tumor growth.

Genomic data

Genomic data was derived from DNA methylation, gene expression, DNA copy number, and microRNA expression, as well as IDH mutation and 1p/19q co-deletion measurement. Specifically, we included six previously identified molecular classifications of LGGs in our analysis:

(1) Molecular subtype based on IDH mutation and 1p/19q co-deletion (three subtypes: IDH mutation-1p/19q co-deletion, IDH mutation-no 1p/19q co-deletion, IDH wild type).
(2) RNASeq cluster (4 clusters: R1–R4).
(3) DNA methylation clusters (5 clusters: M1–M5).
(4) DNA copy number cluster (3 clusters: C1–C3).
(5) microRNA expression cluster (4 clusters: mi1–mi4).
(6) Cluster of clusters (3 clusters: coc1-coc3).

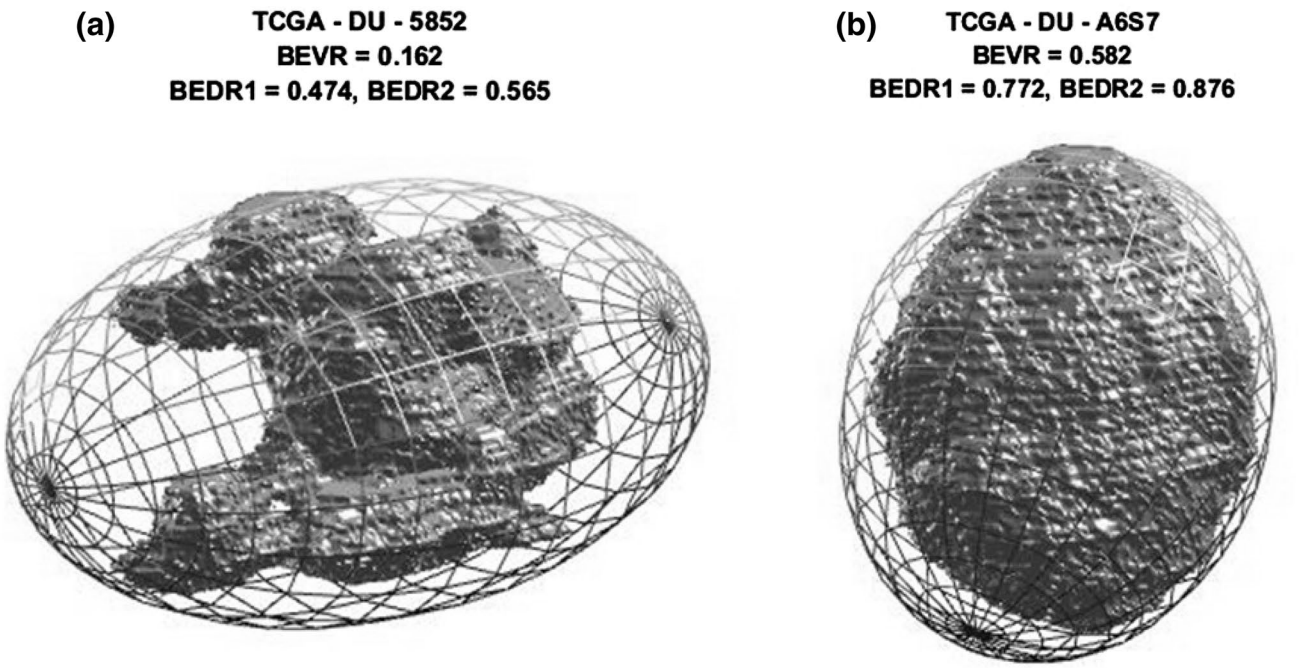

Fig. 1 Illustration of fitting an ellipsoid into a tumor for two tumors with varying level of noncircularity

These classifications were developed in a recent publication defining the molecular landscape of lower-grade gliomas (1). We downloaded the subtype classifications from supplemental materials of that study and correlated them with the imaging data using the unique TCGA identifiers.

Image analysis

FLAIR images were first annotated manually by a researcher in our laboratory by drawing an outline of the FLAIR abnormality on each slice. An in-house MATLAB software program was used for this purpose. The annotations were approved when correct and modified when incorrect by a board eligible radiologist working in our laboratory.

The annotations were used to assess shape features. The features were extracted using computer algorithms developed and implemented in the MATLAB environment in our laboratory. Five features were implemented based on review of literature and discussions between members of our research team about which algorithms would provide a reliable and comprehensive description of the tumor shape [20]. We decided to focus on tumors shape analysis brain following the hypothesis that tumor shape is likely to reflect patterns of tumor growth and underlying genetic composition of the tumor cells as well as patient eventual outcomes. Three of the features were based on a three-dimensional rendering of the tumor using nearest neighbor interpolation between slices. These features are illustrated in Fig. 1. The smallest bounding ellipsoid was algorithmically fit around the tumor such that the entire tumor was contained within the ellipsoid. The Khachiyan algorithm was used for this purpose [21, 22]. If the tumor was comprised of multiple disjoint three dimensional pieces, only the largest component was used for feature calculation. Measurement of this ellipsoid and the relationship with the tumor itself were the basis of the three-dimensional features in our study (detailed features described below). The remaining two features, illustrated in Fig. 2, were based on the FLAIR slice that had the largest FLAIR area and focused on how regular the outline of the abnormality is. The specific five imaging features are listed below:

Bounding ellipsoid volume ratio

The ratio of the FLAIR abnormality volume to the volume of its minimum bounding ellipsoid.

Diameter ratio 1

The ratio of the smallest diameter of the bounding ellipsoid to largest diameter of the bounding ellipsoid. Tumors with a low value of this feature will be elongated or disk-like rather than spherical.

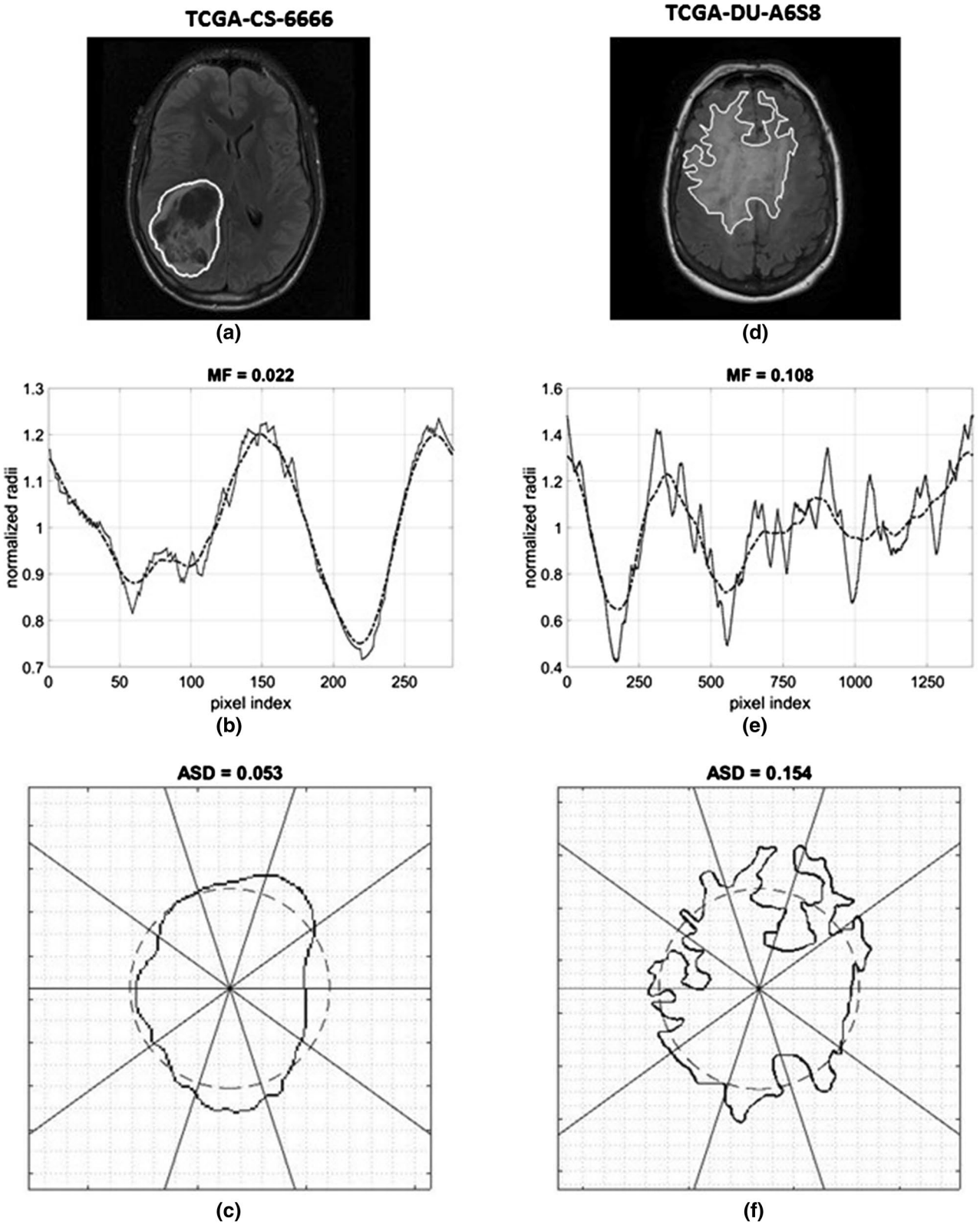

Fig. 2 Illustration of extracting 2D features for 2 lower-grade glioma cases with very different complexity of the tumor shape. Figures **a** and **b** show the FLAIR image for the two cases along with the annotations (*white* outline). Figures **c** and **d** demonstrate extraction of the margin fluctuation feature and figures **e** and **f** demonstrate extraction of the angular standard deviation feature for those cases

Diameter ratio 2

The ratio of the intermediate diameter of the bounding ellipsoid to the largest diameter of the bounding ellipsoid. Tumors with low value of this parameter will tend to be elongated. This feature should be interpreted alongside with the section "Diameter ratio 1".

Margin fluctuation

The standard deviation of the difference between (1) distances of the voxels along the tumor edge from the centroid of the tumor in one slice and (2) the same radial distances, smoothed with an averaging filter with a length equal to 10% of the tumor perimeter in terms of number of pixels. Prior to the calculation of this feature, radial distances are normalized to have a mean of one which removes the impact of tumor size on the value of this feature. This feature quantifies the amount of high frequency changes, i.e., the smoothness, of the tumor boundary. This approach was previously proposed for analysis of spiculation in breast tumors [23, 24].

Angular standard deviation

The average of the radial distance standard deviation across ten equiangular bins in one slice, similar to the one in Georgiou et al. [25]. Prior to the calculation of this feature, radial distances are normalized to have a mean of one. This feature quantifies variation in the tumor margin within relatively small parts of the tumor and captures non-circularity of the tumor.

Statistical analysis

Our primary hypothesis was that there exist associations between the five imaging features and the six genomic subtypes. To assess the association between the genomic subtypes and imaging features, we conducted the Fisher exact test (fisher.test function in R) for each combination of imaging feature (5) and genomic subtype (6). For the purpose of this test, we turned each continuous imaging variable value into a number from 1 to 4 based on which quartile the feature value fell into. For each of the imaging and genomic feature combinations, we used only the cases that had both: imaging and genomic subtype data available.

Since we tested the association of five imaging features with six genomic subtypes, we conducted a total of 30 statistical tests for our primary hypothesis. To account for multiple hypothesis testing, we applied a Bonferroni correction. P-values lower than 0.0017 (0.05/30) were considered statistically significant for our primary radiogenomics hypotheses.

Additionally, we used a heatmap to demonstrate which imaging features were associated with which genomic subtypes as well as a box and whisker plot to show the distribution of the imaging feature value for different subtypes for the imaging feature that showed the strongest association with genomics.

As an additional exploratory analysis, we assessed the association between the imaging variables and patient overall survival. For this purpose, for each imaging variable, we constructed and evaluated a univariate Cox proportional hazards regression model with the imaging feature as the covariate.

Results

Patient characteristics are shown in Table 1. The patient average age was 47 with an almost even split between women and men (56 vs. 53, 1 unknown) in our dataset. Histologically, the tumors were divided between oligodendroglioma (47), astrocytoma (33),

Table 1 Patient and tumor characteristics.

Characteristic	Patients (N = 110)
Age (year)	
Median	47
Range	20–75
Gender	
Female	56
Male	53
Not available	1
Histologic type and grade	
Astrocytoma	
Grade II	8
Grade III	25
Oligoastrocytoma	
Grade II	14
Grade III	15
Oligodendroglioma	
Grade II	29
Grade III	18
Not available	1
IDH-1p/19q subtype	
IDH mutation, 1p/19q co-deletion	26
IDH mutation, no 1p/19q co-deletion	56
IDH wild type	25
Not available	3

Median and range are reported for age. Age for one patient was missing and was ignored in the calculation

and oligoastrocytoma (29). Histology of one tumor was unknown. The data included grade II (51) and grade III (58) tumors with grade of one tumor unknown.

We found the strongest association between the angular standard deviation and the genomic subtypes. Specifically, this imaging features was associated with the IDH-1p/19q subtype ($p < 0.0017$), RNASeq cluster ($p < 0.0002$), copy number cluster ($p < 0.001$), and the cluster of clusters subtype ($p < 0.0002$). There was also an association between the bounding ellipsoid volume ratio and the RNASeq clusters ($p < 0.0005$). The associations between the imaging features and genomic subtypes are illustrated in Fig. 3.

Figure 4 shows distribution of angular standard deviation across different molecular classifications. In the plots, one can see that the high values of angular standard deviation in MRI is associated with IDH wild type subtype and RNASeq R2 subtype both of which are associated with notably poorer prognoses. Angular standard deviation also showed the ability of distinguishing the C2 from C1 and C3 clusters for the CNC classification and coc2 from coc1 and coc3 clusters for the cluster of clusters classification.

When both the ASD and the IDH-1p/19q subtypes are split into two classes (genomic subtype as IDH wild type vs. other and ASD by median), the sensitivity of detecting the IDH wild type subtype by the imaging feature was 0.8, and the specificity was 0.6.

Finally, in our exploratory analysis of the association between the imaging features and patient overall survival, we found that ASD showed a notable association with outcomes ($p = 0.006$) with BEVR showing marginal association ($p = 0.06$). Other imaging variables did not show significant associations with outcomes. BEVR also showed an association with tumor grade ($p < 0.002$), with marginal association of grade also seen with MF ($p < 0.04$) and ASD ($p < 0.02$). No association of tumor grade with BEDR1 and BEDR2 was observed ($p > 0.3$).

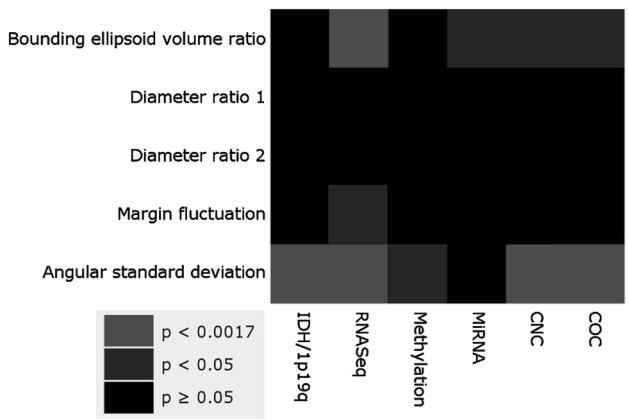

Fig. 3 A heatmap showing associations between the proposed shape measurements and different clusters based on genomic analysis

Discussion

In this multi-institutional, retrospective study with The Cancer Genome Atlas data, we found that previously identified tumor genomic subtypes in lower-grade glioma are strongly associated with the tumor shape as seen in MRI. This strong association shows promise of an imaging-based classification that could potentially replace a more complicated, expensive, and invasive genomic classification while providing similar power in terms of distinguishing patients with different outcomes. This will be particularly useful in unresectable tumors as only tissue from a biopsy (subject to inadequate histologic tumor representation) would be available for genomic subtyping.

Our results show that IDH wildtype tumors demonstrate a notably higher irregularity of the tumor boundary, which is an intuitive result for the following reason: IDH wildtype tumors show a much less favorable prognosis that is comparable with glioblastoma prognosis (1). This is consistent with a more irregular and "invasive" appearance of the tumors. A similar trend was observed for the RNASeq clusters. Specifically, RNASeq R2 cluster showed notably higher values of angular standard deviation as compared with the other clusters. R2 is also associated with dramatically poorer overall survival as compared with R1, R3, and R4 (1). This strongly suggests that angular standard deviation and potentially other shape features could provide prognostic value for patient's outcome. This is currently a topic of research in our laboratory.

With genomic analysis of tumors and an understanding of the contributions of IDH mutation status, TERT promoter mutation status, and 1p/19q co-deletion status, prognostication in lower-grade gliomas has improved above and beyond a basic description of histopathology. Our radiogenomic strategy further supports the previous statement, and we contend that it could further improve prognostication for patients with these tumors. The next steps will be to understand how this strategy can be used to drive treatment decisions. This will be particularly useful when considering aggressive surgery that could lead to neurologic or cognitive dysfunction or radiation therapy that could lead to cognitive dysfunction.

This study focuses on the relationship between shape and tumor molecular subtype. Future work will investigate other aspects of the disease visible in imaging including tumor location, proportions of different tumor components, and tumor texture.

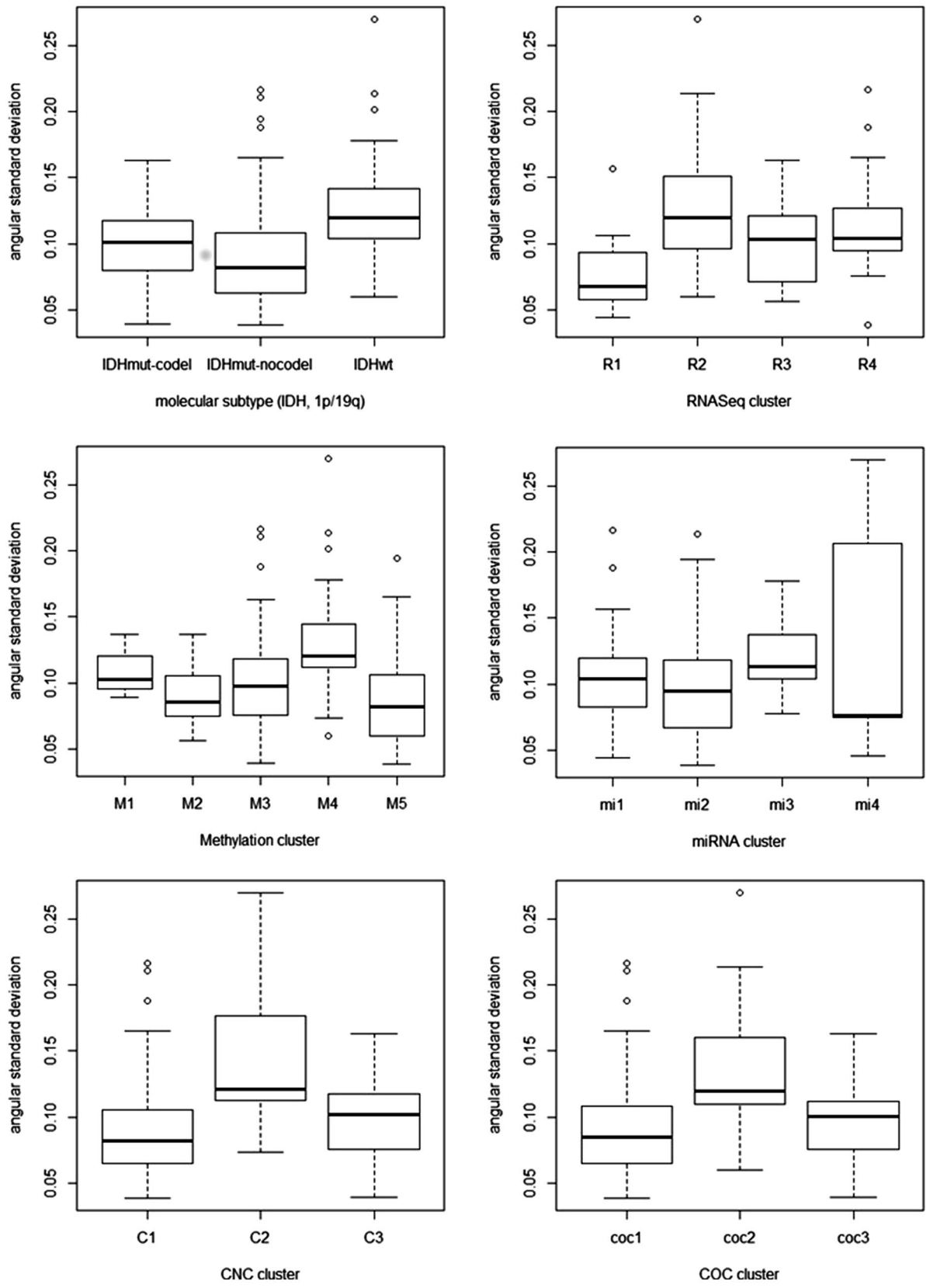

Fig. 4 *Box* and *whisker plots* demonstrating the relationship between different genomics-based clusters and tumor shape as quantified by angular standard deviation

Funding There are no funding sources, which supported this research, to be disclosed.

Compliance with ethical standards

Conflict of interest Dr. Katherine B. Peters received research funding from the following companies: Agios, AMGEN, BioMimetix, Eisai, Genentech, Merck, VBL. Dr. Katherine B. Peters is on the Advisory Board of the following companies:Agios, Novocure. Other authors have nothing relevant to disclose.

Ethical approval This study has been conducted using the publicly available data from The Cancer Genome Atlas (TCGA) and we secured an institutional review board exemption for studying this data at our institution.

Informed consent This study has been conducted using the publicly available data from The Cancer Genome Atlas (TCGA) and the policies for informed consent of TCGA are available at http://cancergenome.nih.gov/abouttcga/policies/informedconsent and http://cancergenome.nih.gov/pdfs/TCGA_Human_Subjects_Protection_and_Data_Access_Policies_Rev_2014-01-16.pdf.

Appendix 1

Full list of the 110 patient IDs used in this study (comma-separated):

TCGA-CS-4941, TCGA-CS-4942, TCGA-CS-4943, TCGA-CS-4944, TCGA-CS-5393, TCGA-CS-5395, TCGA-CS-5396, TCGA-CS-5397, TCGA-CS-6186, TCGA-CS-6188, TCGA-CS-6290, TCGA-CS-6665, TCGA-CS-6666, TCGA-CS-6667, TCGA-CS-6668, TCGA-CS-6669, TCGA-DU-5849, TCGA-DU-5851, TCGA-DU-5852, TCGA-DU-5853, TCGA-DU-5854, TCGA-DU-5855, TCGA-DU-5871, TCGA-DU-5872, TCGA-DU-5874, TCGA-DU-6399, TCGA-DU-6400, TCGA-DU-6401, TCGA-DU-6404, TCGA-DU-6405, TCGA-DU-6407, TCGA-DU-6408, TCGA-DU-7008, TCGA-DU-7010, TCGA-DU-7013, TCGA-DU-7014, TCGA-DU-7018, TCGA-DU-7019, TCGA-DU-7294, TCGA-DU-7298, TCGA-DU-7299, TCGA-DU-7300, TCGA-DU-7301, TCGA-DU-7302, TCGA-DU-7304, TCGA-DU-7306, TCGA-DU-7309, TCGA-DU-8162, TCGA-DU-8163, TCGA-DU-8164, TCGA-DU-8165, TCGA-DU-8166, TCGA-DU-8167, TCGA-DU-8168, TCGA-DU-A5TP, TCGA-DU-A5TR, TCGA-DU-A5TS, TCGA-DU-A5TT, TCGA-DU-A5TU, TCGA-DU-A5TW, TCGA-DU-A5TY, TCGA-EZ-7264, TCGA-FG-5962, TCGA-FG-5964, TCGA-FG-6688, TCGA-FG-6689, TCGA-FG-6690, TCGA-FG-6691, TCGA-FG-6692, TCGA-FG-7634, TCGA-FG-7637, TCGA-FG-7643, TCGA-FG-8189, TCGA-FG-A4MT, TCGA-FG-A4MU, TCGA-FG-A60K, TCGA-HT-7473, TCGA-HT-7475, TCGA-HT-7602, TCGA-HT-7605, TCGA-HT-7608, TCGA-HT-7616, TCGA-HT-7680, TCGA-HT-7684, TCGA-HT-7686, TCGA-HT-7690, TCGA-HT-7692, TCGA-HT-7693, TCGA-HT-7694, TCGA-HT-7855, TCGA-HT-7856, TCGA-HT-7860, TCGA-HT-7874, TCGA-HT-7877, TCGA-HT-7879, TCGA-HT-7881, TCGA-HT-7882, TCGA-HT-7884, TCGA-HT-8018, TCGA-HT-8105, TCGA-HT-8106, TCGA-HT-8107, TCGA-HT-8111, TCGA-HT-8113, TCGA-HT-8114, TCGA-HT-8563, TCGA-HT-A5RC, TCGA-HT-A616, TCGA-HT-A61A, TCGA-HT-A61B.

References

1. Brat DJ, Verhaak RG, Aldape KD, Yung WK, Salama SR, Cooper LA et al (2015) Comprehensive, integrative genomic analysis of diffuse lower-grade gliomas. N Engl J Med 372(26):2481–2498
2. Louis DN, Ohgaki H, Wiestler OD, Cavenee WK, Burger PC, Jouvet A et al (2007) The 2007 WHO classification of tumours of the central nervous system. Acta Neuropathol 114(2):97–109
3. Lang FF, Gilbert MR (2006) Diffusely infiltrative low-grade gliomas in adults. J Clin Oncol 24(8):1236–1245
4. Stupp R, Mason WP, Van Den Bent MJ, Weller M, Fisher B, Taphoorn MJB et al (2005) Radiotherapy plus concomitant and adjuvant temozolomide for glioblastoma. N Engl J Med 352(10):987–996
5. Eckel-Passow JE, Lachance DH, Molinaro AM, Walsh KM, Decker PA, Sicotte H et al (2015) Glioma groups based on 1p/19q, IDH, and TERT promoter mutations in tumors. N Engl J Med 372(26):2499–2508
6. Zhang C-M, Brat DJ (2016) Genomic profiling of lower-grade gliomas uncovers cohesive disease groups: implications for diagnosis and treatment. Chin J Cancer 35(1):12
7. Tchoghandjian A, Koh MY, Taieb D, Ganaha S, Powis G, Bialecki E et al (2016) Hypoxia-associated factor expression in low-grade and anaplastic gliomas: a marker of poor outcome. Oncotarget. doi:10.18632/oncotarget.8046
8. Viswanath P, Najac C, Izquierdo-Garcia JL, Pankov A, Hong C, Eriksson P et al (2016) Mutant IDH1 expression is associated with down-regulation of monocarboxylate transporters. Oncotarget. doi:10.18632/oncotarget.8046
9. Mazurowski MA (2015) Radiogenomics: what it is and why it is important. J Am Coll Radiol 12(8):862–866
10. Mazurowski MA, Zhang J, Grimm LJ, Yoon SC, Silber JI (2014) Radiogenomic analysis of breast cancer: luminal B molecular subtype is associated with enhancement dynamics at MR imaging. Radiology 273:365–372
11. Grimm LJ, Zhang J, Mazurowski MA (2015) A computational approach to radiogenomics of breast cancer: luminal A and luminal B molecular subtypes are associated with imaging features on routine breast MRI extracted using computer vision algorithms. J Magn Reson Imaging. doi:10.1002/jmri.24879
12. Zinn PO, Majadan B, Sathyan P, Singh SK, Majumder S, Jolesz FA et al (2011) Radiogenomic mapping of edema/cellular invasion MRI-phenotypes in glioblastoma multiforme. PLoS One 6(10):e25451
13. Yamamoto S, Han W, Kim Y, Du L, Jamshidi N, Huang D et al (2015) Breast cancer: radiogenomic biomarker reveals associations among dynamic contrast-enhanced MR imaging, long noncoding RNA, and metastasis. Radiology 275(2):384–392
14. Yamamoto S, Maki DD, Korn RL, Kuo MD (2012) Radiogenomic analysis of breast cancer using MRI: a preliminary study to define the landscape. Am J Roentgenol 199(3):654–663

15. Gutman DA, Cooper LA, Hwang SN, Holder CA, Gao J, Aurora TD et al (2013) MR imaging predictors of molecular profile and survival: multi-institutional study of the TCGA glioblastoma data set. Radiology 267(2):560–569
16. Ashraf AB, Daye D, Gavenonis S, Mies C, Feldman M, Rosen M et al (2014) Identification of intrinsic imaging phenotypes for breast cancer tumors: preliminary associations with gene expression profiles. Radiology 272(2):374–384
17. Czarnek NM, Clark K, Peters KB, Collins LM, Mazurowski MA (2016) Radiogenomics of glioblastoma: a pilot multi-institutional study to investigate a relationship between tumor shape features and tumor molecular subtype. SPIE Med Imaging 97850V–97850V
18. Huse JT, Wallace M, Aldape KD, Berger MS, Bettegowda C, Brat DJ et al (2013) Where are we now? And where are we going? A report from the Accelerate Brain Cancer Cure (ABC2) low-grade glioma research workshop. Neuro Oncol 16(2):173–178
19. Mazurowski MA, Clark K, Czarnek NM, Shamsesfandabadi P, Peters KB, Saha A (2017) Radiogenomic analysis of lower grade glioma: a pilot multi-institutional study shows an association between quantitative image features and tumor genomics. In: SPIE Medical Imaging Conference. doi:10.1117/12.2255579
20. Czarnek N, Clark K, Peters KB, Mazurowski MA (2017) Algorithmic three-dimensional analysis of tumor shape in MRI improves prognosis of survival in glioblastoma: a multi-institutional study. J Neurooncol 1–8
21. Moshtagh N (2005) Minimum volume enclosing ellipsoid. Convex Optim 111:112
22. Khachiyan LG (1980) Polynomial algorithms in linear programming. USSR Comput Math Math Phys 20(1):53–72
23. Giger ML, Vyborny CJ, Schmidt RA (1994) Computerized characterization of mammographic masses: analysis of spiculation. Cancer Lett 77(2):201–211
24. Pohlman S, Powell KA, Obuchowski NA, Chilcote WA, Grundfest-Broniatowski S (1996) Quantitative classification of breast tumors in digitized mammograms. Med Phys 23(8):1337–1345
25. Georgiou H, Mavroforakis M, Dimitropoulos N, Cavouras D, Theodoridis S (2007) Multi-scaled morphological features for the characterization of mammographic masses using statistical classification schemes. Artif Intell Med 41(1):39–55